THE JOURNAL OF PROSTHETIC DENTISTRY

RESEARCH AND EDUCATION

Fracture resistance, trueness, and phase transformation of bar-reinforced and nonreinforced implant-supported fixed complete prostheses made of high-strength zirconia: An in vitro study

Rafat Sasany, DDS, PhD,[a] Sümeyye Salvi, DDS,Ucar,[b] Sultan Merve Uçar, DDS,[c] Seyed Ali Mosaddad, DDS,[d] and Mutlu Özcan, DDS, MSD, PhD[e]

ABSTRACT

Statement of problem. Implant-supported, fixed, complete arch zirconia prostheses have been widely used for edentulous patients; however, the reliability of bar-free designs remains uncertain. High-strength zirconia formulations may enable predictable restorations without bar reinforcement.

Purpose. The purpose of this in vitro study was to evaluate the trueness, fracture resistance, and phase transformation behavior of bar-reinforced and nonreinforced complete arch prostheses fabricated from conventional and high-strength zirconia.

Material and methods. Thirty standardized edentulous maxillary models with 6 implant analogs were assigned to 3 groups (n=10): bar-reinforced conventional zirconia (Katana; K-WB), nonreinforced conventional zirconia (Katana; K-NB), and nonreinforced high-strength zirconia (Ice Plus; ICP-NB). The frameworks were digitally designed, milled, sintered, polished, and glazed. The titanium bar was cemented after airborne-particle abrasion. All specimens underwent mastication simulation with thermocycling. Trueness was assessed by superimposing fabricated frameworks onto digital design datasets, phase transformation was analyzed by X-ray diffraction before and after aging, and fracture resistance was measured using a universal testing machine. Data were analyzed using 1-way ANOVA with post hoc tests for fracture strength and trueness and 2-way repeated-measures ANOVA for phase transformation (α=.05).

Results. ICP-NB exhibited the highest mean ±standard deviation fracture resistance (1700 ±50 N), followed by K-WB (1550 ±45 N) and K-NB (900 ±40 N) (P<.05). ICP-NB showed better external trueness compared with both Katana groups (P<.05). In contrast, K-WB demonstrated the best marginal trueness (P<.05). After thermocycling, K-WB and K-NB exhibited significant tetragonal-to-monoclinic phase transformation, while ICP-NB maintained a predominantly tetragonal phase with minimal change (P>.05).

Conclusions. High-strength zirconia (ICP-NB) complete arch prostheses demonstrated favorable fracture resistance, high trueness, and better resistance to low-temperature degradation than conventional zirconia (K-WB, K-NB), suggesting they are a reliable alternative to bar-reinforced designs. (J Prosthet Dent 2026;135:807.e1-e8)

Implant-supported fixed complete prostheses (ISFCPs) have been considered the standard for edentulous patients, offering predictable functional, esthetic, and psychosocial benefits.[1–4] Rapid advances in digital workflows, including computer-aided design and computer-aided manufacturing (CAD-CAM), have expanded the range of materials and fabrication options for ISFCPs, enhancing precision, efficiency, and cost-effectiveness.[5,6] The selection of prosthetic design and restorative material significantly influences biomechanical behavior, fabrication trueness, material structural stability, and long-term clinical outcomes.[7–13] In digitally assisted dentistry, trueness refers to the degree of correspondence between the geometry of a fabricated object and its original CAD dataset, reflecting the

The authors declare that they have no known competing financial interests or personal relationships that could have appeared to influence the work reported in this paper.

[a]Associate Professor, Department of Prosthodontics, Faculty of Dentistry, Istanbul Biruni University, Istanbul, Turkey.
[b]PhD student, Department of Prosthodontics, Faculty of Dentistry, Istanbul Biruni University, Istanbul, Turkey.
[c]Lecturer, Department of Prosthodontics, Faculty of Dentistry, Istanbul Biruni University, Istanbul, Turkey.
[d]Researcher, Department of Conservative Dentistry and Bucofacial Prosthesis, Faculty of Odontology, Complutense University of Madrid (UCM), Madrid, Spain; and Adjunct Faculty Member, Department of Research Analytics, Saveetha Dental College and Hospitals, Saveetha Institute of Medical and Technical Sciences, Saveetha University, Chennai, India.
[e]Professor, Clinic for Masticatory Disorders and Dental Biomaterials, Center for Dental Medicine, University of Zurich, Zurich, Switzerland.

Clinical Implications

Bar-free, high-strength zirconia frameworks offer clinicians the possibility of delivering a complete arch prosthesis as a single, monolithic structure, thereby eliminating interphases and the risk of bar–framework debonding. This approach reduces laboratory complexity and overall cost.

accuracy of the manufacturing process.[14] Zirconia-based ceramics have gained popularity in complete arch applications because of their excellent mechanical and esthetic properties compared with metal–ceramic prostheses.[15–20] The 2018 ITI Consensus Report emphasized that "implant-supported monolithic zirconia prostheses may be a future option with more supporting evidence," reflecting the growing clinical interest in these restorations.[21–24] Conventional 3 mol% yttria-stabilized tetragonal zirconia polycrystal (3Y-TZP) zirconia offers high flexural strength, low fracture probability, and excellent antagonistic wear behavior while preserving esthetics and surface quality.[25–31]

For durable complete arch rehabilitations, 2 principal approaches are commonly used: bar-supported removable overdentures and ISFCPs.[1,32,33] ISFCPs often incorporate a CAD-CAM-fabricated titanium bar to provide rigidity, toughness, and passive fit across long implant spans and distal cantilevers.[1,7,34,35] Recent digital advances have facilitated the integration of titanium bars with monolithic zirconia frameworks, combining titanium's strength with zirconia's esthetics and biocompatibility.[36–38] Although zirconia ISFCPs demonstrate high survival rates and relatively few prosthetic complications,[1,2,39–41] technical issues such as veneering ceramic chipping, debonding at titanium interfaces, and occasional catastrophic framework fractures have been reported.[42,43] Careful technical and clinical planning remains essential to minimize these risks.[36,44,45] Moreover, zirconia prostheses have still been associated with higher rates of technical complications requiring maintenance and repairs.[2,42,46,47] To overcome these limitations, high-strength zirconia formulations have been developed. Manufactured through hot isostatic pressing (HIP), high-strength zirconia formulations achieve flexural strength values of approximately 1900 MPa, exhibit a fine grain size, and demonstrate enhanced resistance to low-temperature degradation.[18,48] Such properties suggest that high-strength zirconia may provide reliable performance without the need for bar reinforcement.[48] Therefore, the purpose of this in vitro study was to compare the trueness, fracture resistance, and phase transformation behavior of bar-reinforced and nonreinforced complete arch zirconia prostheses fabricated from conventional and high-strength zirconia. The null hypothesis was that no significant differences would be found among the tested groups.

MATERIAL AND METHODS

An edentulous maxillary model (Standard working model series ANA-4; Frasaco) was scanned using a 3-dimensional (3D) desktop scanner (Medit T-Series; Medit Corp), and the data were transferred to a design software program (DentalCAD; exocad GmbH). A priori power analysis with a software program (G*Power 3.1; Heinrich-Heine-Universität) for a 1-way ANOVA (3 groups; $f=0.40$; $\alpha=.05$; power=0.80) indicated 30 specimens (10 per group).[3] Thirty standardized digital maxillary models were virtually constructed, incorporating 6 implant sites symmetrically positioned bilaterally between the central and lateral incisors, between the first and second premolars, and in the first molar regions. The exported standard tessellation (STL) files were printed on a 3D printer (MAX UV; Asiga) using a photopolymer material (Freeprint model; Detax GmbH) at a layer thickness of 50 µm. After postprocessing, which included rinsing with isopropyl alcohol and additional light polymerization according to the manufacturer's instructions, the specimens were dried and inspected for surface irregularities. Six internal-connection titanium implant analogs (IS-II Active, Ø4.0 mm × 11.5 mm; NeoBiotech) were inserted into the planned positions and tightened to 20 Ncm with a calibrated torque wrench (Universal Prosthetic kit; NeoBiotech). Corresponding micro-unit transfer copings (Transfer Impression Coping; NeoBiotech) were used for each implant to ensure precise positioning and parallel alignment of the implant analogs during embedding. A bone-mimicking polyurethane resin (F16; Axson Technologies) with an elastic modulus of 3.6 GPa was poured around the peri-implant regions to form a continuous 2- to 3-mm circumferential "bone" layer. Following implant analog placement, each model was rescanned using a 3D desktop scanner (Medit T-Series; Medit Corp) with an accuracy ≤7 µm. The resulting STL datasets were imported into the CAD software program (DentalCAD; exocad GmbH) and aligned within a standardized coordinate system. Thirty frameworks were designed (DentalCAD; exocad GmbH) and divided into 3 groups (n=10): conventional 3Y-TZP zirconia (Katana Zirconia; Kuraray Noritake) reinforced with a custom-milled titanium bar (Ti-6Al-4V, Grade 5; Zirkonzahn) (K-WB), nonreinforced conventional 3Y-TZP zirconia (Katana Zirconia; Kuraray Noritake) (K-NB), and nonreinforced high-strength 3Y-TZP zirconia fabricated with hot isostatic pressing (Ice Plus Zirconia; Zirkonzahn) (ICP-NB). The main compositional and processing characteristics of the zirconia materials are summarized in Table 1.

Katana zirconia frameworks were milled from partially sintered blanks with a 5-axis milling unit (DWX-52D; DGSHAPE Corp), while ICP-NB frameworks were

Table 1. Composition and processing characteristics of zirconia materials tested

Material	Manufacturer	Composition (wt%)	Processing Method	Yttria Content	Grain Size (μm)	Flexural Strength (MPa)*
Katana Zirconia (3Y-TZP)	Kuraray Noritake	ZrO_2 + 3 mol% Y_2O_3 + HfO_2 <5% + Al_2O_3 <0.5%	Conventional sintering	3Y	0.4–0.6	Approximately 1200
Ice Plus Zirconia (3Y-TZP HIP)	Zirkonzahn	ZrO_2 + 3 mol% Y_2O_3 + HfO_2 <5% + Al_2O_3 <0.2%	Hot isostatic pressing (HIP)	3Y	0.2–0.4	Approximately 1900

*Values provided according to manufacturer data

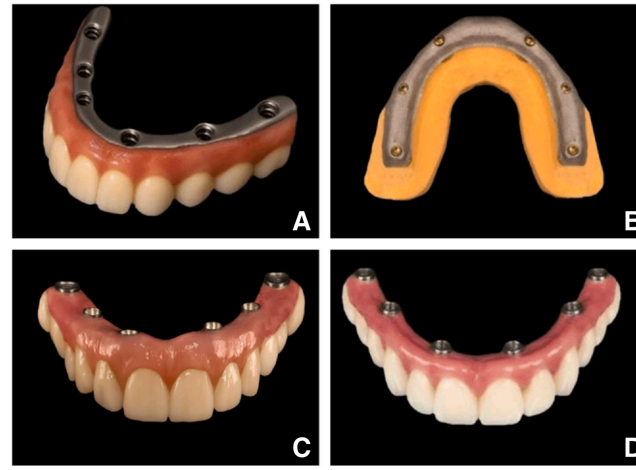

Figure 1. Experimental groups. A, K-WB: bar-reinforced conventional 3Y-TZP zirconia prosthesis (Katana Zirconia; Kuraray Noritake) bonded to titanium bar; B, Custom-milled titanium bar (Ti-6Al-4V, Grade 5; Zirkonzahn); C, K-NB: nonreinforced conventional 3Y-TZP zirconia (Katana Zirconia; Kuraray Noritake); D, ICP-NB: nonreinforced high-strength 3Y-TZP zirconia with hot isostatic pressing (Ice Plus Zirconia; Zirkonzahn).

milled with the manufacturer's dedicated CAD-CAM system. Katana zirconia (Kuraray Noritake) was sintered at a peak temperature of approximately 1550 °C with a total cycle time of 8 hours, including controlled heating and cooling phases. Ice Plus zirconia (Zirkonzahn) was sintered using a HIP-assisted protocol at a peak temperature of approximately 1500 °C, with a prolonged dwell time (up to 120 min) to ensure maximum densification and grain refinement. After sintering, the frameworks were mechanically polished using a sequential protocol with diamond rotary instruments (coarse to fine grit, 40 to 15 μm; Komet Dental) under copious water irrigation. Final surface finishing was performed with zirconia-specific polishing wheels and diamond-impregnated polishing paste (Zirkopol; Komet Dental) until a smooth, glossy surface was obtained. The specimens were then glazed with a thin layer of liquid glaze (Zirkonzahn Glaze; Zirkonzahn) and fired in a porcelain furnace at 800 °C for 7 minutes to standardize the surface finish. The titanium bars were digitally designed in the CAD software program (Detnal CAD; exocad GmbH) by following the same implant dataset used for the zirconia framework design in a horseshoe-shaped configuration with uniform thickness (3 mm) and a height of 4 mm. Each bar was wet milled from titanium blocks using a 5-axis unit (DWX-52D, DGSHAPE Corp), followed by dimensional inspection, sequential silicon carbide polishing (Renfert), and 10-minute ultrasonic cleaning in ethanol (Fig. 1).

In the K-WB group, the intaglio surface of the zirconia frameworks and titanium bars was airborne-particle abraded (Basic quattro; Renfert) with 50-μm aluminum oxide (Korox 50; BEGO) at a 0.2 MPa for 10 seconds from 10 mm, followed by cleaning with oil-free compressed air. Prior to cementation, titanium bars were treated with a universal primer (Monobond Plus; Ivoclar AG). Custom-milled titanium bars were bonded to the intaglio surface of their corresponding zirconia superstructures using a dual-polymerizing resin cement (Multilink Automix; Ivoclar AG). The cement was dispensed into the intaglio surface of the zirconia frameworks, the bars were seated under finger pressure, and excess cement was removed. The margins were tack-polymerized for 2 to 3 seconds with a light-emitting diode (LED) polymerizing unit (Bluephase G2; Ivoclar AG), and final polymerization occurred through dual-polymerizing as per the manufacturer's protocol. Straight multi-unit abutments (2 mm cuff height, 0 degrees angulation; Multi Unit Abutment; NeoBiotech) were tightened to a final torque of 20 Ncm using a calibrated torque wrench (Universal Prosthetic kit; NeoBiotech) according to the manufacturer's recommendations. For frameworks, a diagonal or cross-tightening sequence was applied (from central to distal implants bilaterally), and all screws were retightened to 20 Ncm after 10 minutes to compensate for the settling effect.[14] Screw access channels were sealed with polytetrafluoroethylene (PTFE) tape and restored incrementally with a nanohybrid composite (Filtek Z250 XT; 3M ESPE), light-polymerizing each layer for 40 seconds using an LED unit (Bluephase G2; Ivoclar AG).

Trueness was evaluated by rescanning each fabricated framework (Medit T-Series; Medit Corp) and superimposing it onto the original CAD design using an inspection software program (Geomagic Control X; 3D Systems). After manual pre-alignment, superimpositions were performed using the software's best-fit algorithm. Root mean square (RMS) deviation values were calculated, and color-coded deviation maps were generated to assess both external and marginal trueness. Phase transformation was assessed using X-ray diffraction (XRD) (Bruker D8 Advance; Bruker Corp) with CuKα radiation (λ=1.5406 Å) operated at 40 kV and 40 mA. Diffraction patterns were collected over a 2θ range of 20 to 40 degrees with a step size of 0.02 degrees and a counting time of 1 seconds per step. Peaks corresponding to tetragonal $(101)_t$ at approximately 30.2 degrees, monoclinic $(-111)_m$ at approximately 28.2 degrees, and $(111)_m$ at approximately 31.5 degrees were identified and used to calculate monoclinic phase content according to the Garvie–Nicholson method.[49] Representative diffraction patterns were plotted, and monoclinic phase content (%) was quantified before and after thermocycling to assess susceptibility to low-temperature degradation (LTD).

All specimens underwent mastication simulation in a dual-axis simulator (CS-4.8; SD Mechatronik GmbH) at 1.5 Hz, under a load range of 50 to 250 N at 37 °C. Thermocycling was simultaneously performed between 5 °C and 55 °C for 1 200 000 cycles, with a dwell time of 30 seconds and a transfer time of 10 seconds. For fracture resistance testing, specimens were mounted in a custom metal device and loaded in a universal testing machine (Shimadzu AGS-X; Shimadzu Corp) with the occlusal plane aligned perpendicular to the loading axis (tolerance ≤0.5 degrees). A Ø6-mm hardened steel ball was used to apply a vertical load at the central fossa of the first molar at a crosshead speed of 1 mm/minute until fracture. To homogenize stress distribution, a 1-mm-thick copper foil (4 mm^2 surface area) was interposed between the indenter and the occlusal surface. Fracture load (N) was defined as the first sharp drop in the load-displacement curve.

Statistical analysis was performed with a software program (IBM SPSS Statistics, v28.0; IBM Corp). Normality and homogeneity were assessed with the Shapiro–Wilk and Levene tests. Fracture strength and trueness (external and marginal RMS) were compared using 1-way ANOVA with the Tukey HSD or, when variances were unequal, Welch ANOVA with Games–Howell. Phase transformation was evaluated with 2-way repeated-measures ANOVA (Group × Time) and, when assumptions were violated, change scores (post–pre) analyzed with the Welch 1-way ANOVA or Kruskal–Wallis (α=.05). Results are reported as mean ±SD or median [IQR] with effect sizes and 95% confidence intervals.

RESULTS

Fracture strength, trueness, and phase transformation results are summarized in Tables 2 and 3. For external trueness, ICP-NB exhibited the lowest deviation values, indicating significantly better adaptation than both Katana groups (*P*<.05, Table 2). In contrast, K-WB demonstrated the best marginal trueness, with significantly lower deviations at the prosthesis margins compared with K-NB and ICP-NB (*P*<.05, Table 2). Fracture strength also differed significantly among groups (*P*<.05, Table 2). ICP-NB achieved the highest resistance, followed by K-WB and K-NB, and post hoc analysis confirmed significant differences in all comparisons. Color maps revealed group-specific deviation patterns (Fig. 2). ICP-NB showed predominantly green distribution, reflecting minimal deviation and better external trueness. K-WB displayed more uniform green along margins, indicating improved marginal fit. K-NB exhibited broader color deviations, reflecting greater misfit at both marginal and external levels.

Representative diffraction patterns showed tetragonal peaks in all groups and monoclinic peaks in

Table 2. Fracture resistance and trueness (external and marginal RMS) of complete arch zirconia prostheses fabricated from Ice Plus (ICP-NB) and Katana zirconia (K-WB, K-NB) and one-way ANOVA results for effect of Group

Group	External RMS (µm)	Marginal RMS (µm)	Fracture Resistance (N)	ANOVA F (df)	η^2	*P*
ICP-NB	25.0 ±2.5[a]	45.5 ±4.0[b]	1700 ±50[a]	External: F(2,27)=65.4	0.68	<.05
K-WB	32.5 ±3.0[b]	38.0 ±3.5[a]	1550 ±45[b]	Marginal: F(2,27)=71.2	0.70	<.05
K-NB	35.5 ±3.2[b]	46.2 ±4.2[b]	900 ±40[c]	Fracture: F(2,27)=122.8	0.82	<.05

Values presented as mean ±standard deviation. Different superscript letters within same column indicate statistically significant differences (Tukey post hoc test, α=.05). ICP-NB, nonreinforced high-strength zirconia; K-WB, bar-reinforced conventional zirconia; K-NB, nonreinforced conventional zirconia.

Table 3. Monoclinic phase content (Vm %) of zirconia prostheses before and after thermocycling and two-way repeated-measures ANOVA for effects of Group and Time

Descriptive Values (Mean ±SD)			
Material	**Before TC (Vm %)**	**After TC (Vm %)**	**Within-group *P****
K-WB	1.2 ±0.5	11.5 ±1.8	<.05
K-NB	1.0 ±0.4	12.0 ±2.0	<.05
ICP-NB	0.9 ±0.3	2.8 ±0.7	>.05
Two-way repeated-measures ANOVA results			
Effect	F(df)	η^2	*P*
Time (pre → post)	F(1,27)=84.6	0.76	<.05
Group	F(2,27)=18.9	0.58	<.05
Group × Time	F(2,27)=16.3	0.55	<.05

*Within-group *P* values indicate differences before and after thermocycling within each group. ICP-NB, nonreinforced high-strength zirconia; K-WB, bar-reinforced conventional zirconia; K-NB, nonreinforced conventional zirconia; TC, thermocycling; Vm, monoclinic phase content.

Katana zirconia after thermocycling (Fig. 3). XRD revealed significant effects of Time and Group (*P*<.05), with monoclinic content increasing after thermocycling (1.0 ±0.4% to 8.8 ±5.1%). K-WB (6.4 ±5.7%) and K-NB (6.5 ±6.0%) showed higher monoclinic content than ICP-NB (1.8 ±1.1%). A significant Group × Time interaction (*P*<.05) confirmed differing transformation levels. Post hoc comparisons showed a marked increase in monoclinic content for both K-WB and K-NB after thermocycling (*P*<.05), whereas ICP-NB maintained a predominantly tetragonal phase with no significant change (*P*>.05, Table 3).

DISCUSSION

The null hypothesis that no significant differences would be found among the tested groups was rejected, as Ice Plus zirconia without bar reinforcement demonstrated the highest fracture resistance and excellent phase stability, while bar-reinforced Katana zirconia achieved better marginal trueness. The higher fracture resistance observed for Ice Plus zirconia can be explained by its microstructural characteristics. Ice Plus is processed using HIP, which increases density, reduces porosity, and refines grain size, thereby improving crack resistance and flexural strength.[48] These properties enhance the material's ability to withstand tensile stresses and delay catastrophic crack propagation,[18] which is particularly critical in ISFCPs that are subject to

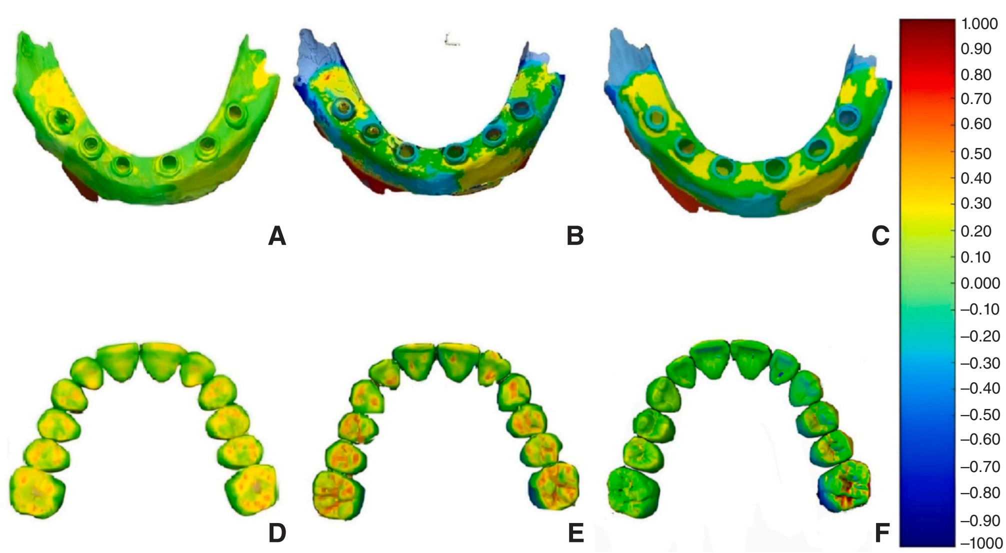

Figure 2. Color-coded deviation maps of trueness. A, Marginal trueness of ICP-NB; B, Marginal trueness of K-WB; C, Marginal trueness of K-NB; D, External trueness of ICP-NB; E, External trueness of K-WB; F, External trueness of K-NB. *Green areas* indicate minimal deviation with better adaptation, whereas *red and blue areas* reflect positive and negative misfits, respectively.

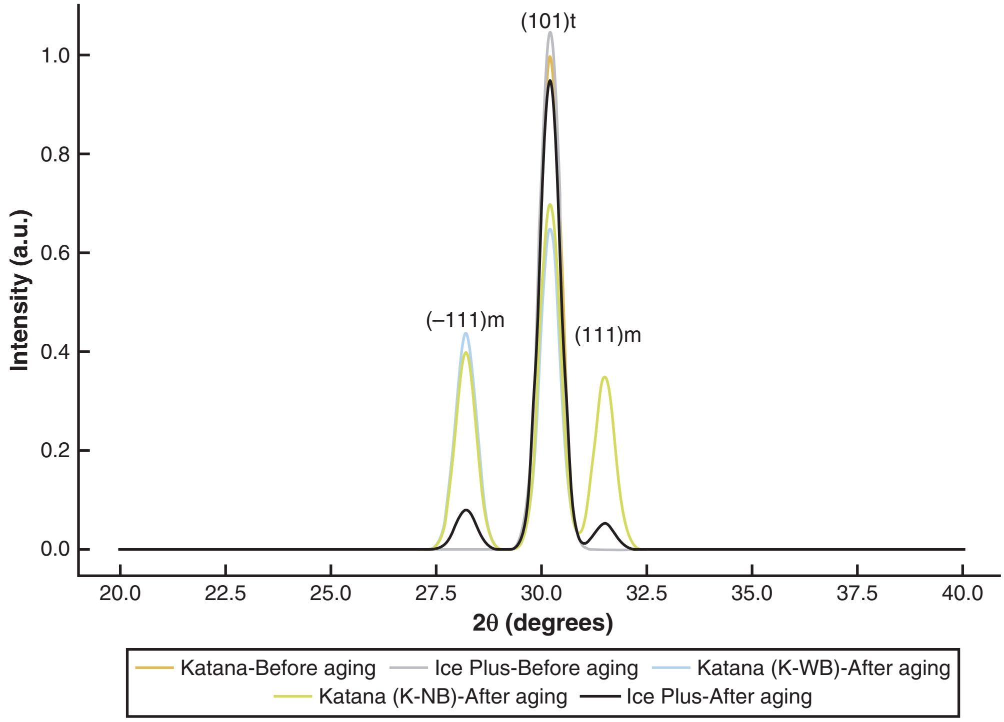

Figure 3. Representative X-ray diffraction patterns showing tetragonal and monoclinic peaks used for phase transformation analysis. K-WB, bar-reinforced conventional 3Y-TZP zirconia prosthesis (Katana Zirconia; Kuraray Noritake) bonded to titanium bar; K-NB, nonreinforced conventional 3Y-TZP zirconia (Katana Zirconia; Kuraray Noritake); Ice Plus, nonreinforced high-strength 3Y-TZP zirconia with hot isostatic pressing (Ice Plus Zirconia; Zirkonzahn).

long-span loading.[8] By comparison, bar-reinforced Katana zirconia achieved a similarly high resistance because the bonded titanium bar redistributed functional stresses along the framework, limiting flexural deformation and reducing the risk of bulk fracture.[36] The significantly lower fracture strength of nonreinforced Katana zirconia underscores the limitations of conventional zirconia formulations when used in long-span monolithic configurations without additional support, as they are more susceptible to crack initiation and unstable crack growth under loading.[6,18] Clinically, the high resistance values recorded for Ice Plus and bar-reinforced Katana exceed reported maximum bite forces (500 to 900 N),[11,12] supporting their suitability for clinical function. However, in patients with parafunctional habits, the higher strength of Ice Plus zirconia may offer added protection against failure.

In terms of trueness, Ice Plus zirconia demonstrated the lowest external deviation, reflecting better overall trueness than both Katana groups, potentially because of reduced distortion during milling and sintering, as HIP processing minimizes sintering shrinkage variability and produces more stable frameworks.[19] Precise external accuracy reduces strain accumulation at the implant–framework interface, minimizing the risk of screw loosening or implant component fracture.[7] However, bar-reinforced Katana zirconia exhibited the best marginal trueness, likely because of the rigid titanium bar acting as a stabilizer during bonding, which reduced marginal discrepancies.[9] This highlights a trade-off: nonreinforced HIP zirconia offers excellent global trueness, whereas bar reinforcement optimizes marginal fit. From a clinical perspective, the magnitude of misfit observed in the present study remained well within reported acceptable thresholds. Marginal discrepancies below approximately 120 μm have been generally considered clinically acceptable,[14,37,44] and similar misfit levels have been associated with acceptable bone changes.[4,45] Both bar-reinforced and nonreinforced zirconia frameworks showed deviations well below this threshold, suggesting that the statistically significant differences are unlikely to have adverse clinical consequences. Nonetheless, zirconia's higher Young modulus (200 GPa) compared with titanium (100 GPa)[14] means it accommodates strain less effectively, making precise adaptation essential to avoid stress concentration at the screw–abutment interface. These results indicate that both HIP zirconia and bar-reinforced zirconia can achieve clinically acceptable adaptation.

The phase transformation results revealed significant tetragonal-to-monoclinic conversion in both Katana groups after thermocycling, whereas Ice Plus zirconia exhibited minimal change. This difference can be explained by the susceptibility of conventional 3Y-TZP to LTD,[26] which is accelerated in the presence of moisture and temperature fluctuations.[27] The volumetric expansion associated with the phase transformation introduces tensile stresses and microcracking, which may ultimately reduce long-term strength.[18] In contrast, the refined microstructure of HIP-processed Ice Plus zirconia confers resistance to LTD by lowering the driving force for transformation and reducing the nucleation of microcracks.[28] Although transformation toughening may provide short-term benefits by inhibiting crack propagation, extended aging has been reported to lead to strength degradation in long-term studies.[20,29–31] Ice Plus zirconia stability suggests greater aging resistance and long-term durability.

Clinically, these findings highlight the benefits of monolithic zirconia frameworks without bar reinforcement. Removing the titanium bar simplifies fabrication, reduces bulk, and eliminates potential adhesive interface failures,[13] while the absence of veneering ceramics avoids chipping. Reported survival rates for monolithic zirconia prostheses range from 88% to 100%, with mostly minor complications.[38,41] The present results indicate that high-strength zirconia, such as Ice Plus, may enhance reliability by combining high fracture resistance, precise adaptation, and LTD resistance with the practical advantages of a monolithic design.

Limitations of this study included the in vitro design using standardized edentulous maxillary models, which did not replicate biological or biomechanical variability. Occlusal dynamics, bone remodeling, and patient-specific parafunction were not simulated, and only short-term thermomechanical aging was applied. Thus, findings should be interpreted with caution.

CONCLUSIONS

Based on the findings of this in vitro study, the following conclusions were drawn:

1. Prostheses made of high-strength HIP zirconia (Ice Plus) achieved better fracture resistance and high trueness compared with bar-reinforced conventional zirconia, supporting its potential use without bar reinforcement.
2. Bar reinforcement improved marginal trueness, reducing discrepancies at the implant–prosthesis interface, while HIP zirconia improved overall external trueness, ensuring better global adaptation.
3. Ice Plus zirconia demonstrated greater stability against low-temperature degradation than conventional Katana zirconia, suggesting a lower risk of aging-related weakening in long-term function.

REFERENCES

1. Bidra AS. Complete arch monolithic zirconia prosthesis supported by cobalt chromium metal bar: A clinical report. *J Prosthodont*. 2020;29:558–563.
2. Bidra AS, Tischler M, Patch C. Survival of 2039 complete arch fixed implant-supported zirconia prostheses: A retrospective study. *J Prosthet Dent*. 2018;119:220–224.
3. Gonçalves FCP, Amaral M, Borges ALS, et al. Fracture load of complete-arch implant-supported prostheses reinforced with nylon-silica mesh: An in vitro study. *J Prosthet Dent*. 2018;119:606–610.
4. Jemt T, Book K. Prosthesis misfit and marginal bone loss in edentulous implant patients. *Int J Oral Maxillofac Implants*. 1996;11:620–625.
5. Kapos T, Evans C. CAD/CAM technology for implant abutments, crowns, and superstructures. *Int J Oral Maxillofac Implants* 2014(29_):117–136.
6. Selz CF, Vuck A, Guess PC. Full-mouth rehabilitation with monolithic CAD/CAM-fabricated hybrid and all-ceramic materials: A case report and 3-year follow up. *Quintessence Int*. 2016;47:115–121.
7. Mijiritsky E, Elad A, Krausz R, et al. Clinical performance of full-arch implant-supported fixed restorations made of monolithic zirconia luted to a titanium bar: A retrospective study with a mean follow-up of 16 months. *J Dent*. 2023;137:104675.
8. Cabello-Domínguez G, Pérez-López J, Veiga-López B, et al. Maxillary zirconia and mandibular composite resin-lithium disilicate-modified PEEK fixed implant-supported restorations for a completely edentulous patient with an atrophic maxilla and mandible: A clinical report. *J Prosthet Dent*. 2020;124:403–410.
9. Speroni S, Antonelli L, Coccoluto L, et al. The effectiveness and predictability of BioHPP (Biocompatible High-Performance Polymer) superstructures in toronto-branemark implant-prosthetic rehabilitations: A case report. *Prosthesis*. 2025;7:10.
10. Faverani LP, Barão VA, Ramalho-Ferreira G, et al. The influence of bone quality on the biomechanical behavior of full-arch implant-supported fixed prostheses. *Mater Sci Eng C Mater Biol Appl*. 2014;37:164–170.
11. Flanagan D. Bite force and dental implant treatment: A short review. *Med Devices (Auckl*. 2017;10:141–148.
12. Jansen van Vuuren L, Broadbent JM, Duncan WJ, Waddell JN. Maximum voluntary bite force, occlusal contact points and associated stresses on posterior teeth. *J R Soc N Z*. 2020;50:132–143.
13. Rutkunas V, Kules D, Mischitz I, et al. Misfit simulation on implant-supported prostheses with different combinations of engaging and nonengaging titanium bases: Part 3: A radiographic evaluation. *J Prosthet Dent*. 2025;133:222–228.
14. Abou-Ayash S, Schimmel M, Özcan M, et al. Trueness and marginal fit of implant-supported complete-arch fixed prosthesis frameworks made of high-performance polymers and titanium: An explorative in-vitro study. *J Dent*. 2021;113:103784.
15. Stawarczyk B, Taufall S, Roos M, et al. Bonding of composite resins to PEEK: the influence of adhesive systems and air-abrasion parameters. *Clin Oral Investig*. 2018;22:763–771.
16. Carames J, Tovar Suinaga L, Yu YC, et al. Clinical advantages and limitations of monolithic zirconia restorations full arch implant supported reconstruction: Case series. *Int J Dent*. 2015;2015:392496.
17. Wachtel A, Zimmermann T, Sütel M, et al. Bacterial leakage and bending moments of screw-retained, composite-veneered PEEK implant crowns. *J Mech Behav Biomed Mater*. 2019;91:32–37.
18. Kontonasaki E, Giasimakopoulos P, Rigos AE. Strength and aging resistance of monolithic zirconia: An update to current knowledge. *Jpn Dent Sci Rev*. 2020;56:1–23.
19. Cesar PF, Miranda RBP, Santos KF, et al. Recent advances in dental zirconia: 15 years of material and processing evolution. *Dent Mater*. 2024;40:824–836.
20. Lasko G, Danilenko I, Weber U, et al. Numerical study of the effect of residual stresses on fracture toughness in the microstructure of ZrO2 ceramics. *Theor Appl Fract Mech*. 2025;139:105047.
21. Hanawa T. Zirconia versus titanium in dentistry: A review. *Dent Mater J*. 2020;39:24–36.
22. Huang B, Chen M, Wang J, Zhang X. Advances in zirconia-based dental materials: Properties, classification, applications, and future prospects. *J Dent*. 2024;147:105111.
23. Cinquini C, Alfonsi F, Marchio V, et al. The Use of Zirconia for Implant-Supported Fixed Complete Dental Prostheses: A Narrative Review. *Dent J ((Basel))*. 2023;11:144.
24. Morton D, Gallucci G, Lin WS, et al. Group 2 ITI Consensus Report: Prosthodontics and implant dentistry. *Clin Oral Implants Res*. 2018;29(16):215–223.
25. Aldhuwayhi S. Zirconia in dental implantology: A review of the literature with recent updates. *Bioengineering (Basel)*. 2025;12:543.
26. Chevalier J, Gremillard L, Deville S. Low-temperature degradation of zirconia and implications for biomedical implants. *Annu Rev Mater Res*. 2007;37:1–32.
27. Rautenbach Z, Haiek M, Ruales-Carrera E, Özcan M. Phase transformation of yttria-stabilized zirconia after the use of various bur types in dry and wet conditions: A systematic review and meta-analysis. *J Mech Behav Biomed Mater*. 2025;169:107064.
28. Matsui K, Nakamura K, Kumamoto A, et al. Low-temperature degradation in yttria-stabilized tetragonal zirconia polycrystal doped with small amounts of alumina: Effect of grain-boundary energy. *J Eur Ceram Soc*. 2016;36:155–162.
29. Kim JW, Covel NS, Guess PC, et al. Concerns of hydrothermal degradation in CAD/CAM zirconia. *J Dent Res*. 2010;89:91–95.

30. Kim HT, Han JS, Yang JH, et al. The effect of low temperature aging on the mechanical property & phase stability of Y-TZP ceramics. *J Adv Prosthodont*. 2009;1:113–117.
31. Atalay Seçkiner P, Gönüldaş F, Akat B, et al. Investigation of phase transformation and fracture pattern as a result of long-term chewing simulation and static loading of reduced-diameter zirconia implants. *Materials (Basel)*. 2024;17:4719.
32. Candido LM, Miotto LN, Fais L, et al. Mechanical and surface properties of monolithic zirconia. *Oper Dent*. 2018;43:E119–E128.
33. Sadowsky SJ. Treatment considerations for maxillary implant overdentures: A systematic review. *J Prosthet Dent*. 2007;97:340–348.
34. Stumpel LJ, Haechler W. The metal-zirconia implant fixed hybrid full-arch prosthesis: An alternative technique for fabrication. *Compend Contin Educ Dent*. 2018;39:176–181.
35. Jaiswal SB, Jain S, Jain V, et al. Evaluation and comparison of stresses between all-on-4 and all-on-6 treatment concepts with three different prosthetic materials in the maxilla: A finite element analysis study. *Cureus*. 2024;16:e71362.
36. Froimovici FO, Butnăraşu CC, Montanari M, Săndulescu M. Fixed full-arch implant-supported restorations: Techniques review and proposal for improvement. *Dent J ((Basel))*. 2024;12:408.
37. Al-Meraikhi H, Yilmaz B, McGlumphy E, et al. In vitro fit of CAD-CAM complete arch screw-retained titanium and zirconia implant prostheses fabricated on 4 implants. *J Prosthet Dent*. 2018;119:409–416.
38. Marchio V, Cinquini C, Alfonsi F, et al. Retrospective analysis of full-arch zirconia rehabilitations on dental implants: Clinical outcomes and patient satisfaction. *Appl Sci*. 2025;15:416.
39. Chen X, Xu Z, Gai K, et al. Biomechanical analysis of All-on-4 implant supported framework using different materials across various clinical practice. *BMC Oral Health*. 2025;25:552.
40. Papathanasiou I, Kamposiora P, Papavasiliou G, Ferrari M. The use of PEEK in digital prosthodontics: A narrative review. *BMC Oral Health*. 2020;20:217.
41. Rojas Vizcaya F. Retrospective 2- to 7-Year follow-up study of 20 double full-arch implant-supported monolithic zirconia fixed prostheses: Measurements and recommendations for optimal design. *J Prosthodont*. 2018;27:501–508.
42. Jemt T, Henry P, Lindén B, et al. Implant-supported laser-welded titanium and conventional cast frameworks in the partially edentulous law: A 5-year prospective multicenter study. *Int J Prosthodont*. 2003;16:415–421.
43. Sailer I, Karasan D, Todorovic A, et al. Prosthetic failures in dental implant therapy. *Periodontol 2000*. 2022;88:130–144.
44. Yilmaz B, Kale E, Johnston WM. Marginal discrepancy of CAD-CAM complete-arch fixed implant-supported frameworks. *J Prosthet Dent*. 2018;120:65–70.
45. Maceiras L, Liñares A, Nóvoa L, et al. Marginal changes at bone-level implants supporting fixed screw-retained partial implant prostheses with or without intermediate standardised abutments: 1-year results of a randomised controlled clinical trial. *Clin Oral Implants Res*. 2023;34:263–274.
46. Degidi M, Nardi D, Piattelli A. Immediate definitive rehabilitation of the edentulous patient using an intraorally welded titanium framework: A 3-year prospective study. *Quintessence Int*. 2010;41:651–659.
47. Svanborg P, Stenport V, Eliasson A. Fit of cobalt-chromium implant frameworks before and after ceramic veneering in comparison with CNC-milled titanium frameworks. *Clin Exp Dent Res*. 2015;1:49–56.
48. Zirkonzahn. ICE Plus zirconia: Zirkonzahn; 2025 [updated September 25, 2025. Accessed September 25, 2025:[Available from: ⟨https://zirkonzahn.com/en/products/millable-materials/ice-plus⟩.
49. Garvie RC, Nicholson PS. Phase analysis in zirconia systems. *J Am Ceram Soc*. 1972;55:303–305.

Corresponding author:
Dr Seyed Ali Mosaddad
Department of Conservative Dentistry and Bucofacial Prosthesis
Faculty of Odontology
Complutense University of Madrid (UCM)
Plaza Ramón y Cajal, s/n
Ciudad Universitaria, Madrid 2804
SPAIN
Email: semosadd@ucm.es

CRediT authorship contribution statement

Rafat Sasany: Conceptualization, Methodology, Software, Formal analysis, Validation, Investigation, Resources, Data curation, Writing – review and editing, Visualization, Supervision, Project administration. **Sümeyye Salvi:** Methodology, Validation, Writing – review and editing, Investigation, Formal analysis, Project administration. **Sultan Merve Uçar:** Software, Formal analysis, Investigation, Data curation, Writing – original draft preparation. **Seyed Ali Mosaddad:** Investigation, Writing – review and editing, Visualization. **Mutlu Özcan:** Validation, Writing – review and editing, Formal analysis, Project administration.

https://doi.org/10.1016/j.prosdent.2025.11.033